Electric and hybrid propulsion systems using fractional slot permanent magnet brushless machines and drives

Prateek , Singhal. Department of Electronics, Lucknow.

Research Article

Date of Submission: 2-04-2025 Date of Acceptance: 5-05-2025 Date of Publication: 1-06-2025

Abstract: In recent years, research has focused on fractional slot permanent magnet brushless machines with concentrated non-overlapping windings. Because of their high torque density, high efficiency, low torque ripple, excellent flux-weakening, and fault-tolerance characteristics, they have already been used in commercial HEVs. However, when an inside PM rotor is used, the reluctance torque component is generally low or even insignificant, and such machines show comparatively high rotor eddy current loss, possibly large unbalanced magnetic force, acoustic noise, and vibration owing to rich mmf harmonics. Their many structural and design elements for EV/HEV applications are collected in this study.

Keywords: imbalanced magnetic force, vibration, cogging torque, fault tolerance, flux weakening, fractional slot, iron loss, magnet loss, modular construction, permanent magnet machines, and winding inductance.

Introduction

Electric (EV) and hybrid electric (HEV) cars are made possible in large part by electrical machineries and drives. The fundamental requirements for these applications are as follows [1]–[3]: (a) High torque density and power density; (b) High torque for starting, at low speeds and hill climbing, and high power for high speed cruising; (c) Wide operating speed range; (d) High efficiency over wide speed and torque ranges, especially at low torque operation; and (e) Intermittent overload capability for brief periods of time.

PM brushless machines have been widely employed for EV/HEV applications because of their inherent efficiency due to the permanent magnet (PM) excitation. In order to maximize torque density and minimize torque pulsation, they can be broadly categorized as either brushless DC (BLDC), where the desired back-emf waveform is trapezoidal and the current waveform is controlled to be rectangular, or brushless AC (BLAC), where the desired back-emf waveform is sinusoidal and the current waveform is controlled to be sinusoidal. However, because of their benefits in terms of torque density, economy, and controllability, BLAC drives are often preferred in EV/HEV applications [4][5].

Recent studies have focused on surface-mounted PM (SPM) brushless machines with a concentrated non-overlapping winding and a fractional number of slots per pole [6]–[66]. The stator coils may be coiled on every tooth (double-layer winding) or on every other tooth (single-layer winding). They feature excellent flux-weakening and fault-tolerance performance [35]–[45], short end windings that result in a low copper loss, high efficiency, and a high power density, as well as an intrinsically low cogging torque [46]–[51]. On the other hand, the permanent magnets and a high stator space harmonic mmf interact to produce the torque. Relatively large rotor eddy current loss [54]–[59], perhaps significant imbalanced magnetic force [60]–[61], acoustic noise and vibration [62]–[66], etc., may be caused by the fundamental and low order space harmonic mmfs that spin in relation to the rotor. Furthermore, when an internal PM (IPM) rotor is used, the reluctance torque component is either insignificant or very low. For EV/HEV applications, this document outlines the different structural and design elements of fractional-slot SPM machines.

Permanent Magnet Brushless Machines

Because of its great efficiency and torque density, PM BLAC machines are already used in commercial HEVs. For instance, the University of Sheffield designed a 3-phase, 24-slot, 22-pole PM BLAC machine for a supercapacitor-based electrical torque boost system for cars with downsized internal combustion engines [14].

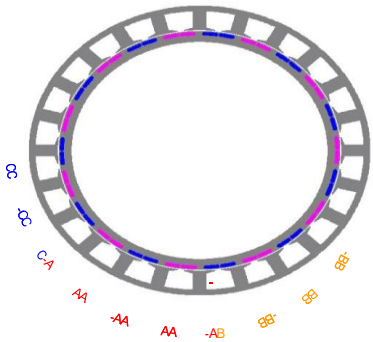


Fig. 1. 3-phase, 24-slot, 22-pole, PM BLAC machine with modular stator winding and IPM rotor [14]. Rated output power=18.5kW, rated speed=1700rpm, rated torque=105Nm. (a) Cross-section of 3-phase, 24-slot, 22-pole IPM BLAC machine,

(b) Machine test rig.

2.1 Slot and Pole Number Combinations Table I lists the most common combinations of slot number Ns and pole number 2p when concentrated stator windings are used, as well as the number of slots per pole per phase q=1 or q=0.5, as well as 2p=Ns±1 and 2p=Ns±2, despite the fact that there are many possible slot number and pole number combinations for PM brushless machines.

TABLE I

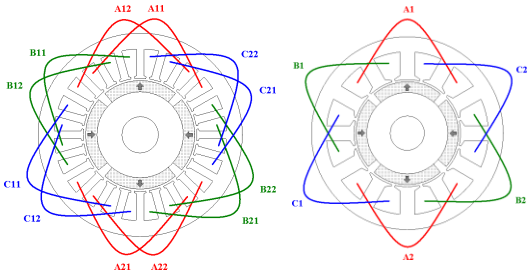
FEASIBLE SLOT/POLE COMBINATIONS FOR 3-PHASE PM CONCENTRATED WINDING BRUSHLESS MACHINES

FOR WHICH Q=1, Q=0.5, $N_S=2P \pm 1$ AND $N_S=2P \pm 2$

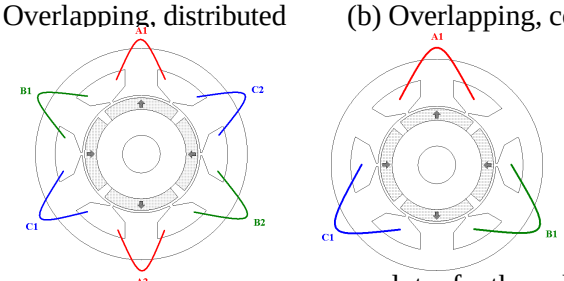
Number of poles, 2p	Feasible slot number			
	q=1	q=0.5	$N_S = 2p\pm1$	$N_S = 2p\pm2$
2	6	3	3	-
4	12	6	3	6
6	18	9	-	-
8	24	12	9	6
10	30	15	9	12
12	36	18	-	-
14	42	21	15	12
16	48	24	15	18
18	54	27	-	-
20	60	30	21	18
22	66	33	21	24
24	72	36	-	-
26	78	39	27	24
28	84	42	27	30
30	90	45	-	-
32	96	48	33	30
34	102	51	33	36
36	108	54	-	-
38	114	57	39	36
40	120	60	39	4

42	126	63	-	-
44	132	66	45	4
46	138	69	45	48

For 3-phase overlapping concentrated winding brushless machines, q=1, Fig. 2(b), e.g. $N_s/2p$=6/2, 12/4, 18/6, 24/8, 30/10, 36/12,
42/14, etc. In the conventional 3-phase fractional slot brushless machines which employ concentrated non-overlapping stator windings, the most common combinations of slot number N_s and pole number $2p$ are of ratio 3/2, i.e. q=0.5, Fig.2(c), e.g. $N_s/2p$=3/2, 6/4,
9/6, 12/8, 15/10, 18/12, 21/14, etc. They are widely used as BLDC motors in the spindle drives and fans. In such machines, if an IPM rotor is employed reluctance torque component still exists.
In order to maximize the flux-linkage and torque density, it is desirable for the coil-pitch to be as close to the pole-pitch as possible. Therefore, N_s and $2p$ should differ by the smallest possible integer, e.g. by only one, i.e.$2p=N_s\pm1$. In this case, typical slot/pole combinations for 3-phase machines are $N_s/2p$=3/2, 3/4; 9/8, 9/10; 15/14, 15/16; 21/20,
21/22, etc. Due to the fractional ratio of slot number to pole number, a huge least common multiple between the number of slots and poles, and a maximum common divider of 1, the cogging torque in such machines is quite modest. As will be covered in more detail in section 4.4, one drawback of such machines is that they may display an unbalanced magnetic force because of the diametrically asymmetric arrangement of the stator slots and coils [6]. This could shorten the bearing life and cause excessive vibration and acoustic noise.
Hence, in practice, the most appropriate slot and pole numbers are related by $2p=N_s\pm2$. For a balanced 3-phase machine, typical $N_s/2p$ combinations are 6/4, 6/8; 12/10, 12/14; 18/16, 18/20; 24/22, 24/26, etc.
It is worthy to note that as the pole number increases, the feasible slot numbers which result in high winding factor and hence high flux-linkage increase.



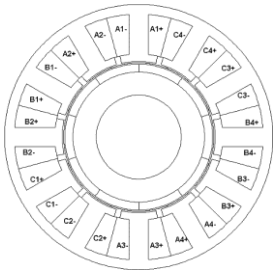
(a) Overlapping, distributed (b) Overlapping, concentrated



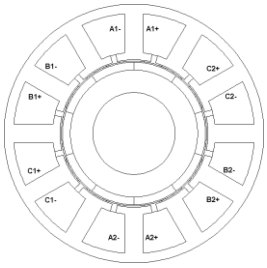
advantages. Although there are a lot of other slot and pole number combinations, they are similar in principle.
The number of stator slots must be even if a single layer winding, or alternating tooth wound topology, is used. Furthermore, Ns/(4t), where t is the largest common divider between the slot number and pole number, must be an even number to prevent an imbalanced magnetic force caused by the axially asymmetric arrangement of the stator coils.
Since the magnet has a relative permeability that is similar to that of air and the effective airgap is the sum of

the real airgap length and the magnet thickness, the armature reaction field is often minimal in SPM machines and the stator windings have a low inductance. As a result, SPM machines typically have a lower capacity for flux-weakening than IPM machines. However, in SPM machines with alternating teeth and a fractional number of slots per pole, the phase windings are effectively isolated both physically and magnetically. By using the relatively large slot leakage flux, a high per-unit self-inductance can be easily achieved to realize a "infinite" flux-weakening capability and to limit the potential short-circuit current.
The likelihood of a phase-to-phase failure is reduced by the coils' physical isolation and the little mutual inductance between phases. As a result, these machines may have far more fault tolerance and flux-weakening capacity than more traditional PM machine designs.

Non-overlapping, all teeth
wound



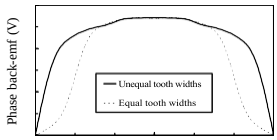
Non-overlapping, alternate teeth wound
Fig. 2. Stator winding dispositions.
2.2. All and Alternate Teeth Wound (Double-and Single-Layer Windings)
In some machines, such as 2p=Ns±2, a coil may be carried by either all the teeth (double-layer winding) or just alternating teeth (single-layer winding), as seen in Figs. 2 and 3, respectively. In [13], the electromagnetic performance of machines with such windings was evaluated in terms of the back-emf, the cogging torque, and the winding inductances. This comparison revealed that machines with just alternate teeth wound may provide some performance.
(a) All teeth wound (double-layer winding)



(a) Alternate teeth wound (single-layer winding)
Fig. 3 12-slot/10-pole machines having all and alternate teeth wound.

Unequal Tooth Structure
The tooth widths may become uneven when only alternate teeth are wrapped [27][28]. The benefit of using unequal tooth widths is examined in this section in machines with various slot and pole number combinations. The performance difference between machines with equal and unequal tooth widths decreases, meaning that the advantages of using unequal tooth widths gradually decrease as the pole number increases because of the inter-pole leakage flux.
However, 2p=Ns±2. Both equal and unequal tooth widths are studied, with Ns/2p ranging from 6/4 and 6/8 to 18/16 and 18/20. Open-circuit field distributions for 6/4 and 12/10 machines are shown in Fig. 4.

10



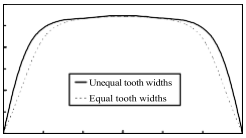
5

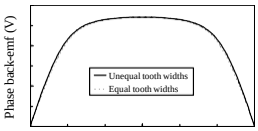
0
0 90 180
Angular position (elec. deg)
Angular position (elec. deg)
Irrespective of whether a machine has equal or unequal tooth widths, a non-overlapping winding has unity coil-distribution factor. However, the coil-pitch factors are different. A machine with equal tooth widths has a coil-

(a) 6-slot/4-pole (b) 6-slot/8-pole

15

10





5

0
0 90 180
pitch = $2\pi p/N_s$, and, hence, an effective coil-
0 90 180
Angular position (elec. deg)
Angular position (elec. deg)
pitch factor is less than one, i.e. $K_{pn}=sin(np\pi/N_s)$, where n is the order of the harmonic. For a machine with unequal tooth widths the tips of the wound teeth can be dimensioned such that they almost span a pole-

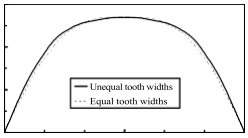
15

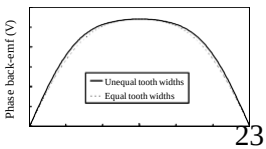
Phase back-emf (V)

10

5

0
12-slot/10-pole (d) 12-slot/14-pole
15



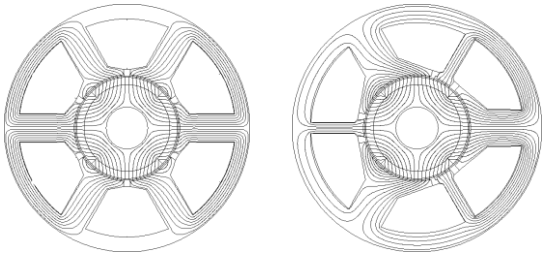


10

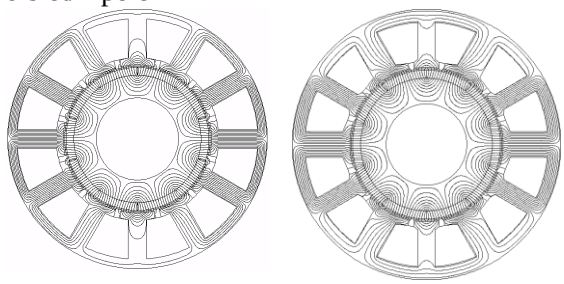
5

0
0 90 180
pitch, so that unity pitch factor and maximum
0 90 180
Angular position (elec. deg)
Angular position (elec. deg)

flux-linkage per coil are obtained. Consequently, in general, the phase back-emf waveform which results with unequal tooth widths is more trapezoidal, as evidenced in Fig. 5.



Equal tooth widths (b) Unequal tooth widths
6-slot/4-pole



(a) Equal tooth widths (b) Unequal tooth widths
12-slot/10-pole

Fig. 4 PM brushless machines with equal and unequal tooth widths.

However, as the pole number increases, inter-pole leakage flux increases. As a consequence, the airgap flux density distribution and the back-emf waveform of the machines with unequal width teeth both become more sinusoidal, Fig. 5. Ultimately,

18-slot/16-pole (f) 18-slot/20-pole Fig. 5 Phase back-emf waveforms.

Modular Stator

This stator architecture [29] is a kind of brushless machine where all teeth are wrapped, the slot and pole numbers are linked by 2p=Ns±2, and the tooth widths are identical (Fig. 3(a)). As shown in Fig. 6 for a 12-slot/10-pole machine, the primary difference is the removal of alternating parts of the stator back-iron. Two coils are coiled on neighboring teeth with opposing priorities, as shown in Fig. 3(a). The bulk of the armature reaction field is limited to these two neighboring teeth and the stator back-iron between them, as can be shown later in Fig. 9(a). The neighboring stator back-irons, on the other hand, get relatively little flux. As a result, these parts of the stator back-iron may be deleted, and the stator will consist of a collection of segmented and mechanically separated "U"-shaped cores (Fig. 6(a)). It should be noted that the stator back-iron thickness in traditional brushless machines with a single piece of stator lamination and pole and slot numbers related by 2p=Ns±2 is typically about half of the tooth body width because the maximum flux that flows in a single tooth will be nearly equally divided into the two sides of the back-iron, Fig. 3. On the other hand, with the segmented stator back-iron machine design, the flux

is restricted to flow in this U-shaped magnetic circuit, Fig. 6(b), coming from the rotor magnets. Therefore, in order to prevent magnetic saturation, the back-iron of the U-shaped segment must be bigger than the original and should be raised to be equivalent to the tooth body width. This has the drawback of reducing the slot area (by 28% in this particular instance), which raises the current density and increases the copper loss. Alternatively, the outer diameter must be raised if the slot area remains same.

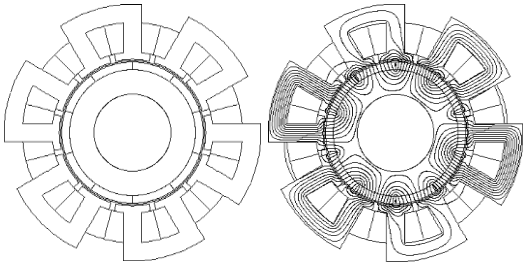
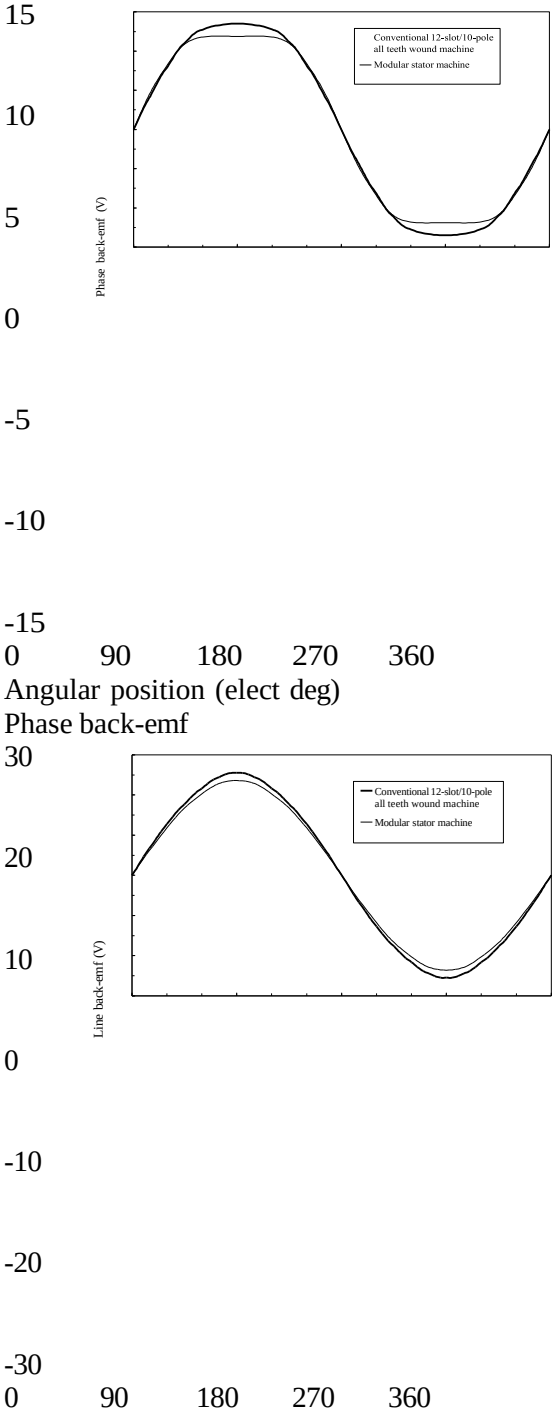


Fig. 6 12-slot/10-pole modular stator machine.



Angular position (elect deg)
Line back-emf
Fig. 7 Finite element predicted phase and line back-emf waveforms at 400rpm in 12-slot/10-pole machine.

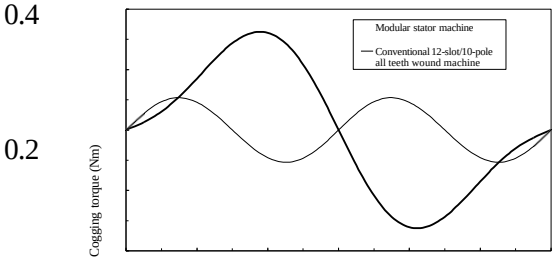


Fig. 8 Finite element predicted cogging torque in 12-slot/10-pole machine.

Finite element projected phase and line back-emf waveforms for the 12-slot/10-pole modular stator machine are shown in Fig. 7. Phase and line back-emf waveform peaks are only somewhat lower than those of the original 12-slot/10-pole all-teeth wound machine. Additionally, as can be observed by contrasting Fig. 4(IIa) for the 12-slot/10-pole all teeth wrapped machine and Fig. 6 for the modular stator machine, the open-circuit field distribution is significantly changed by segmenting the stator core. This most likely explains why the modular stator machine's peak cogging torque is higher (Fig. 8).

Interior PM Rotor

When an IPM rotor is used in fractional slot IPM machines, the reluctance torque is often minimal or even reduced. Additionally, both the stator iron loss and the electromagnetic loss in the IPM rotor might be substantial [30, 31]. The main benefits of employing an IPM rotor are simple rotor magnet retention and a reasonably large winding inductance to enhance flux weakening efficacy. An overlapping stator winding is often necessary to use the saliency torque in an IPM machine, as shown in Figs. 2(a) and (b). A dispersed overlapping winding, on the other hand, has longer end windings, which compromises the torque density and increases copper loss. If both are properly constructed, the torque density of SPM and IPM machines is often relatively comparable.

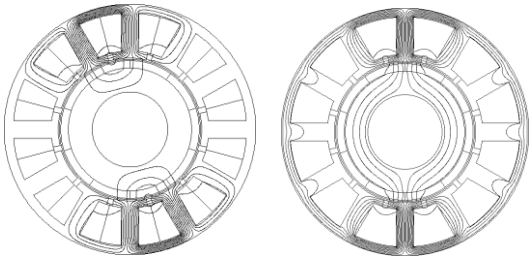
Machine Parameters and Control Performance

Winding Inductances

The winding inductances of motors with all teeth wound and those with just alternating teeth wound vary most significantly [32]–[34]. The armature reaction field distributions for the two winding dispositions vary dramatically, as shown in Fig. 9 for 10-pole, 12-slot machines. Consequently, the motor with simply alternating teeth has a lot greater self-inductance than the motor with all teeth carrying a coil, and the mutual-inductance between phases is substantially lower. Nevertheless, compared to the 15-slot/10-pole motor, which has q=0.5, the self-inductances of both motors are much larger. The self- and mutual inductances for

additional motors with varied slot and pole combinations but the same performance criterion are shown in

Table II.



(a) All teeth wound (b) Alternate teeth wound Fig. 9. Field distributions with phase A excited.

TABLE II SELF- AND MUTUAL-INDUCTANCES (mH) [13]

Motor	All teeth wound		Alternate teeth wound	
	L	M	L	M
12-slot/10-pole	3.03	-0.34	4.64	0.0023
12-slot/14-pole	2.34	-0.23	3.68	0.0028
18-slot/16-pole	1.86	-0.11	2.63	0.0031
18-slot/20-pole	1.43	-0.12	2.17	-0.009
24-slot/22-pole	1.37	-0.071	1.80	0.0014
24-slot/26-pole	1.10	-0.058	0.83	0.000

Flux-Weakening Capability

It is generally known [35][36] that when a PM brushless machine is built with 1.0 per-unit d-axis inductance, it may attain the maximum flux-weakening capacity, which is defined as the ratio of the maximum speed to the base-speed, under supply inverter voltage and current limits.

fulfill equation (1), even for SPM machines with a relatively low Ld and a high ⁹m. For instance, an SPM machine with "infinite" flux-weakening capability was achieved in [37] and in [38]–[40] with only alternating stator teeth wound, where the winding inductance is comparatively higher due to larger slot leakage and airgap harmonic leakage, as covered in section 3.1.

Fault-Tolerant Performance

By using the relatively high airgap inductance and the leakage flux at the slot openings, it is easy to achieve a high per-unit self-inductance to limit the potential short-circuit current in alternating teeth wound PM machines (single-layer winding), which effectively isolate the phase windings both magnetically and physically. The likelihood of a phase-to-phase failure is reduced by the coils' physical isolation and the little mutual inductance between phases. As a result, their fault tolerance may be far greater than that of more traditional machine designs, much like the flux-weakening capabilities [41][45].Under flux-weakening control, the maximum speed can be several times higher than the base speed. However, when operated in the awhere $\square_m$ is the stator flux-linkage due to the magnets, L_d is the d-axis inductance, and I_r is the rated current.

Although it is possible to design a PM brushless machine which satisfies the foregoing requirement, generally, for most PM machines $L_dI_r/\square_m<1$, since the d-axis inductance is relatively low as a consequence of the recoil permeability of the magnets being approximately equal to 1.0. Nevertheless, in this case the higher the ratio of $L_dI_r/\square_m$ the higher will be the flux-weakening capability, which, theoretically, is 'infinite' when the ratio is 1.0. However, the higher the flux-linkage $\square_m$ to achieve a high low-speed torque capability, the more difficult it is to realize wide speed operation.

In [35], it was shown that it was possible to

high voltage, viz. the induced emf, which is much higher than the dc link voltage, since the demagnetizing

current component is removed. Therefore, there is a possibility of a catastrophic fault on both the PM machine and its drive due to the high voltage and the associated regenerative power. One of the possible ways is to short-circuit the motor by simply switching all three upper switches off and all three lower switches on, or vice verse, without causing an excessive winding current for a properly designed permanent magnet motor.

At high speeds, the effect of winding resistance can be neglected. Consequently, the steady-state short-circuit current is predominately along the d-axis and tending to a constant, i.e.

design any PM brushless machine to achieve 'infinite' flux-weakening capability. Clearly,

$$I_a \approx \frac{E_m}{x_d} = \frac{\psi_m}{L_d} \quad (2)$$

however, if the rated current is high (e.g. the machine is liquid cooled), it is much easier to For an ideally designed motor which has an infinite field weakening capability, i.e.

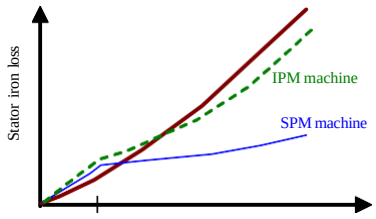
$\psi_m = L_d I_r$, the short circuit current will be limited to the rated current.

Parasitic Effects

Cogging Torque

The interaction between the stator teeth and the rotor permanent magnets produces cogging torque. Because the stator slots are positioned at different relative circumferential positions with respect to the edges of the iron loss as the degree of flux-weakening increases, using a fractional number of slots per pole not only increases the fundamental order but also decreases the amplitude of the cogging torque [52]. Because the armature response field has a larger harmonic content owing to the tiny effective airgap, IPM machines often have a much greater full-load iron loss, which may be equivalent to or even higher than the no-load iron loss [52][53].

Open-circuit



magnets [46]-[51]. In general, the higher the least common multiple between the number of

Base-speed

Speed (per-unit)
poles and the number of slots,
N_{scm} , the lower
Fig. 11. Variation of iron loss in SPM and IPM machines when
the cogging torque, while the smaller the greatest common divider between the number of poles and the number of slots, the lower the cogging torque.
For example, the smallest common multiple N_{scm} □ 30 for the 15-slot/10-pole motor, while N_{scm} □ 60 for the 12-slot/10-pole motors. Hence, very low cogging can be achieved
their open-circuit stator iron losses are designed to be the same.
Rotor Eddy Current Loss
Rotor magnet eddy current loss may cause significant heating of the magnets, due to the relatively poor heat dissipation from the rotor. In turn, this may result in partial irreversible demagnetization, particularly of sintered NdFeB magnets, which have relatively high temperature coefficients of remanence and

when $2p \square N_S \square 2$, as shown in Fig. 10. The coercivity and a moderately high electrical

lowest cogging is achieved with machines conductivity. It is particularly important to

having $2p \square N_S \square 1$, albeit with high unbalanced magnetic force, as will be further discussed in section 4.4.

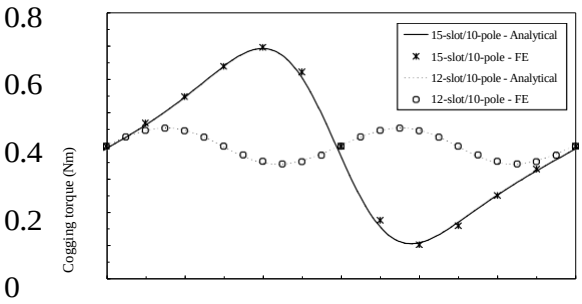


Fig. 10. Cogging torque waveforms.

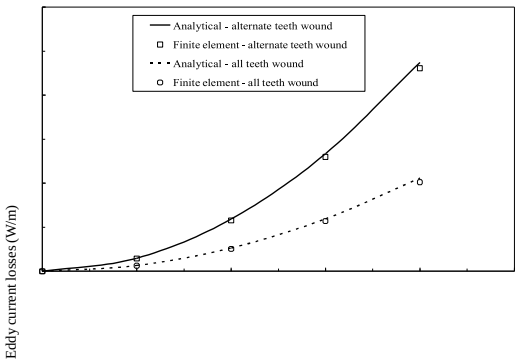
Iron Loss

The full-load iron loss in the constant torque working range is typically 20–50% greater, but the no-load iron loss rises with rotational speed due to the fixed PM excitation. However, as shown in Fig. 11, the machine topology determines the iron loss that occurs under load in the flux-weakening mode. Consider the rotor magnet eddy current loss in fractional-slot PM machines, which exhibit very rich spatial mmf harmonics [54]–[59] that are not in synchronization with the rotor rotational speed. In general, SPM machines may have lower full-load iron loss, and despite the increase in fundamental frequency, it usually becomes much lower than the no-load.

The magnet loss variation of 10-pole, 12-slot fractional slot PM machines at rated current for BLAC and BLDC operations under the same load state is shown in Fig. 12 [57]. The square of the rotor's rotating speed increases the eddy current loss. It is almost twice as high in alternate teeth wound machines as it is in all teeth wound machines. Additionally, because of temporal harmonics, BLDC operation causes a far larger eddy current loss than BLAC operation. The magnet loss for the combination of this space harmonic and the fundamental time harmonic for all three motors is zero because the electromagnetic torque is generated by the fifth space harmonic (mmf), which spins in synchronism with the rotor. The magnet loss related to the fundamental component of the phase current is relatively minor when all the teeth are wrapped (Fig. 13(a)). The 5th and 7th space harmonic mmf and the 5th and 7th current time harmonics account for the bulk of the loss. On the other hand, when alternate teeth are wrapped, the loss is mostly caused by the fundamental, fifth, and seventh current time harmonics, as well as the fundamental and seventh space harmonic mmfs,

Figs. 13(b).

60

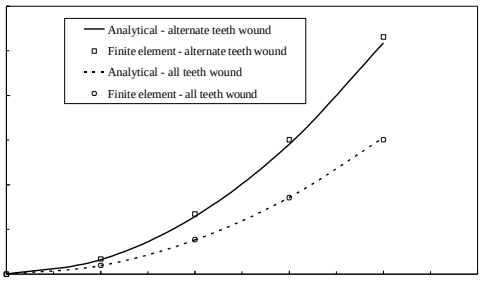


40

20

The eddy current loss is influenced significantly by the maximum current density, or electric loading, the loss varying approximately in proportion to the square of the current density and rotor speed.
If the loss is unacceptable it may be reduced by segmenting the magnets, either circumferentially or axially, or both. With the increase of the number of circumferential segments per pole on the eddy current loss is almost reduced inversely proportional to the square of number of magnet segments. Segmentation is proven to be very effective in reducing the loss.
0

120



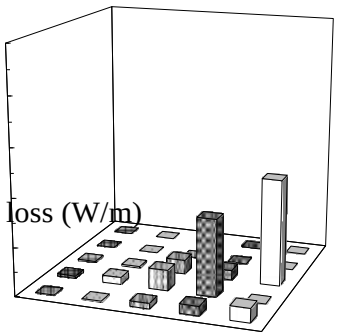
80 Eddy current losses (W/m)

Unbalanced Magnetic Force

The axially asymmetric arrangement of the stator slots and coils results in an imbalanced magnetic force even in the absence of rotor eccentricity [60][61]. As an illustration [60],

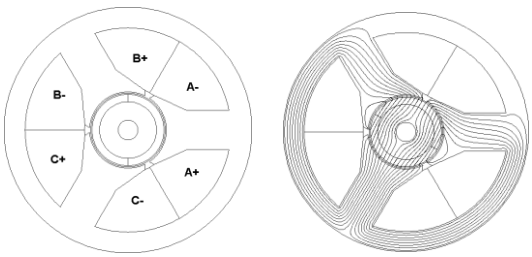
Fig. 14 depicts the open-circuit, armature reaction, and resulting field distributions of the 3-slot/2-pole machine under idealized current waveforms with an amplitude of 10A, and Fig. 15 contrasts the variation of the unbalanced magnetic force as calculated by FE and analytically predicted. It is evident that the impact of the diametrically asymmetric placement of

Fig.12. Variations of eddy current losses with rotor speed at rated current.

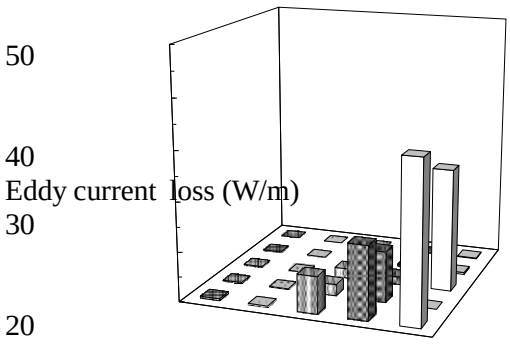


stator slots on the unbalanced magnetic force is relatively small, and the unbalanced magnetic force in BLDC mode is slightly higher than in BLAC mode. The average unbalanced magnetic force increases almost linearly with the load.

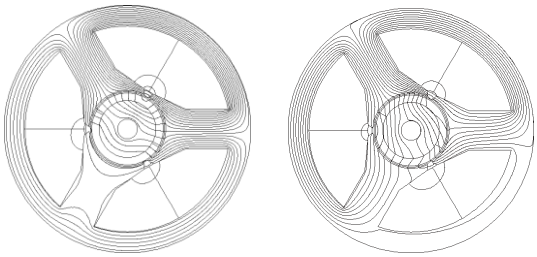
10 13
11
7
0 5



Space
13 11
7 5
1 harmonics, *v*
1



Winding disposition (b) Open-circuit



(c) Armature reaction (d) Resultant

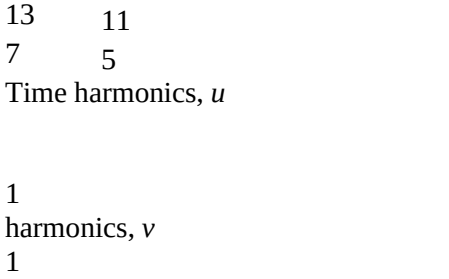


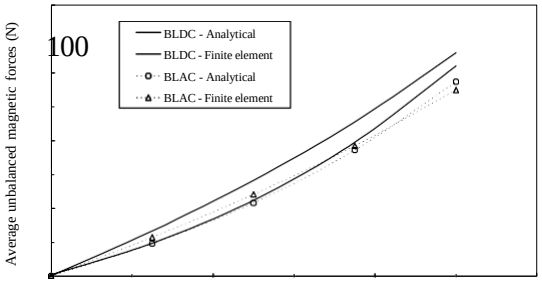
Fig.14. Disposition of phase windings and open-circuit, armature reaction, and resultant field distributions for 3-slot/2-pole

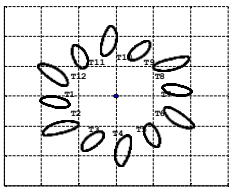
Alternate teeth wound
Fig. 13. Loss spectra at 1600rpm, BLDC mode.
machine in BLDC mode, (ia=-1A, ib=10A and ic=0A).

00
150

150

100 600 400





50

0

-50

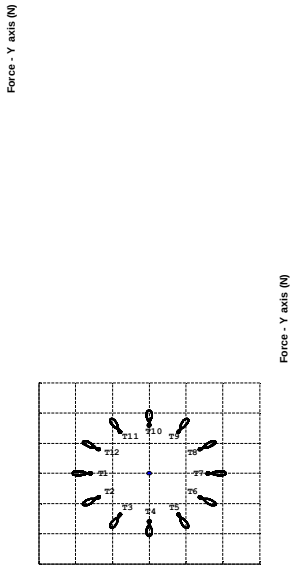
-100

50

0

-50

-100



200

-150
-150 -100 -50 0 50 100 150
Force - X axis (N)

-150
-150 -100 -50 0 50 100 150
Force - X axis (N)

0
0 4 8 12
Phase current (A)
(a) No load (b) Full load
Fig. 16. FE predicted tooth force loci.

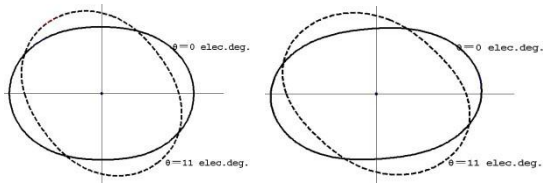


Fig. 15. Variation of average unbalanced magnetic force with phase current for 3-slot/2-pole machine.

Acoustic Noise and Vibration

High vibration and acoustic noise will result if the radial vibration force frequency matches the natural frequency of the stator mechanical structure with the same order of vibration mode. The radial vibration force frequency for variable speed drives will fluctuate over a very broad range, making it almost difficult to prevent mechanical resonance. However, because of the comparatively high mechanical stiffness of the stator, the mechanical response and the related radiated acoustic noise will be minimal if the vibration mode order associated with the main radial exciting force is intended to be high [62]. Therefore, it is crucial to examine the lowest vibration mode order, which is greatly impacted by the combinations of slot and pole numbers in fractional slot PM machines.

The electromagnetic energy that affects every

(a) No load (b) Full load

Fig. 17. FE predicted fundamental radial tooth force distribution.

FAdditional analyses [64]–[66] reveal that for integer-slot PM machines, q=1, 2, 3,..., the dominant radial force is primarily caused by the fundamental magnet field itself, and the dominant vibration mode order is equal to pole number, 2p, which is typically high and, as a result, the noise and vibration are typically low. The interaction between the harmonic in the magnet field and the harmonic in the armature reaction field, however, is the primary source of the dominant radial force in all fractional-slot PM machines. On the other hand, noise and vibration increase with load and can be much higher because the dominant vibration mode order can be as low as 1 or 2, which strongly depends on the slot and pole number combinations as well as the winding topologies, e.g.

stator tooth can be predicted from the finite

For

$2p \square N_S \square 2$

machines having double-

element (FE) analysis, using the Maxwell stress method. Fig. 16 shows the resulting layer winding, the lowest order of radial force harmonic is 2.

force loci for all the teeth, T1~T12, of 12-slot,

For

$2p \square N_S \square 2$

machines having single

10-pole, and 3-phase BLAC motor on no-load

and full-load, respectively. The frequencies of vibration and noise in integer-slot and fractional-slot PM machines are the same, being multiples of the fundamental, $f=2pf_1$, where f_1 is the rotor rotation frequency [62][64][65].

From FE predicted tooth forces, the corresponding electromagnetic vibration can be derived using a vibration model, while the corresponding acoustic noise can be obtained from the acoustic radiated model [62]. However, the vibration mode order, Fig. 17, can be simply determined from the mode order of radial force since they are the same.

layer winding, the lowest order of radial force harmonic is also 2 if N_s/t is even, where t is the greatest common divider between N_s and $2p$. However, for machines with N_s/t= odd, the lowest order of radial force harmonic is 1.

For $2p \square N_S \square 1$ machines, the lowest order of radial force harmonic is 1.

For q=0.5 machines, the lowest radial force harmonic is equal to pole-pair number, p.

Conclusions

High torque density, high efficiency, low torque ripple, excellent flux-weakening, and fault-tolerance performance are characteristics of fractional slot PM brushless machines with concentrated non-overlapping windings. Slot and pole number combinations, all and alternate tooth wound (double- and single-layer windings), equal and unequal tooth structure, modular stator, machine parameters and control performance, such as winding inductances, flux-weakening, and fault-tolerant performance, as well as parasitic effects,

such as rotor eddy current loss, unbalanced magnetic force, and acoustic noise and vibration, have all been summarized in this paper for EV/HEV applications.

References

[1] C.C. Chan: "The cutting edge of fuel cell, electric, and hybrid vehicles," IEEE Proceedings, Volume 95, Issue 4, pages 704-718, 2007.
[2] Z. Q. Zhu and D. Howe, "Electrical machines and drives for electric, hybrid, and fuel cell vehicles," IEEE Proceedings, Volume 95, Issue 4, pages 746-765, 2007.
[3] Z.Q. Zhu and C.C. Chan, "Electrical machine topologies and technologies on electric, hybrid, and fuel cell vehicles," IEEE Vehicle Power and Propulsion Conf. (VPPC), Keynote Speech-KN3, 3-5 September 2008, Paper No. H08787, pp. 1-6.
[4] Z.Q. Zhu, J.X. Shen, and D. Howe, "Flux-weakening characteristics of trapezoidal back-EMF PM machines in brushless DC and AC modes," Journal of Asian Electrical Vehicles, vol.4, no.2, pp.919-925, 2006.
[5] Z.Q. Zhu, Y.F. Shi, and D. Howe, "Comparison of torque-speed characteristics of interior-magnet machines in brushless ac and dc modes for EV/HEV applications," Journal of Asian Electrical Vehicles, vol.4, no.1, pp.843-850, 2006.
[6] "Design of brushless permanent magnet motors," J.R. Hendershot and T.J.E. Miller, Magna Physics Publishing & Clarendon Press, 1994.
[7] IEEE Trans. on Industry Applications, vol. 30, no. 5, pp. 1258-1266, 1994; C. C. Chan, J. Z. Jiang, G. H. Chen, X. Y. Wang, and K. T. Chau, "A novel polyphase multipole square-wave permanent magnet motor drive for electric vehicles."
[8] "Synthesis of high performance PM machines with concentrated windings," J. Cros and P. Viarouge, IEEE Trans. on Energy Conversion, vol. 17, no. 2, pp. 248–253, 2002.
[9] "Winding factors and Joule losses of permanent magnet machines with concentrated windings," F. Magnussen and C. Sadarangani, Proceedings of the International Electric Machines and Drives Conference (IEMDC), Madison, USA, June 1-4, 2003, pp. 333-339.
[10] F. Magnussen, P. Thelin, and C. Sadarangani, "Performance evaluation of permanent magnet synchronous machines with concentrated and distributed windings including the effect of field-weakening," IEE International Conference on Power Electronics and Electrical Machines (PEMD), vol. 2, pp. 679-685, 2004.
[11] "Performance analysis of fractional slot wound PM-motors," Proceedings of the International Conference on Electrical Machines (ICEM), paper no. 509, 2004, P. Salminen, J. Mantere, J. Pyrhonen, and M. Niemela.
[12]P. Salminen, M. Niemela, and J. Pyrhonen, "Performance analysis of fractional slot wound PM-motors for low speed applications," IEEE Industry Applications Society Conf., vol. 2, pp. 1032-1037, 2005.
[13]
"Comparison of PM brushless motors, with either all or alternative wound teeth," D. Ishak, Z.Q. Zhu, and D. Howe, IEEE Trans. on Energy Conversion, vol.21, no.1, pp.95-103, 2006.
[14] "Three-phase modular permanent magnet brushless machine for torque boosting on a downsized ICE vehicle," J. B. Wang, Z. P. Xia, and D. Howe, IEEE Trans. Vehicular Technology, vol.54, no.3, pp.809-816, 2005.
[15] IEEE Trans. on Vehicular Technology, vol.57, no.5, pp.2714-2720, 2008; J. B. Wang, K. Atallah, Z. Q. Zhu, and D. Howe, "Modular 3-phase permanent magnet brushless machines for in-wheel applications."
[16] Analysis of surface PM machines with fractional-slot concentrated windings by A.M. El-Refaie, T.M. Jahns, and D. Novotny, IEEE Trans. Energy Conversion, vol.21, no.1, pp. 34-43, 2006.
[17] IEEE Trans. on Energy Conversion, vol., no. 1, pp. 53-60, 2008; A.M. EL-Refaie and T. M. Jahns, "Impact of winding layer number and magnet type on synchronous surface PM machines designed for wide constant-power speed range operation."
[18] N. Bianchi, "Fractional-slot PM Machine Theory and Design," CLEUP, 2007.

[19] "Synthesis of high performance PM motors with concentrated windings," N. Bianchi, S. Bolognani, and G. Comelato, IEEE Trans. on Energy Conversion, vol.17, no.2, pp.248-253, 2002.
[20] N. Bianchi and M. Dai Pre, "Using the star of slots in designing fractional-slot single-layer synchronous motors," IEE-EPA, vol. 153, no. 3, pp. 459-466, 2006.
[21]N. Bianchi, S. Bolognani, M. D. Pre, and G. Grezzani, "Design considerations for fractional-slot winding configurations of synchronous machines," IEEE Trans. on Industry Applications, vol. 42, no. 4, pp. 997-1006, 2006.
[22]N. Bianchi, S. Bolognani, and M. D. Pre, "Magnetic loading of fractional-slot three-phase PM motors with non-overlapped coils," IEEE Trans. on Industry Applications, vol.44, no.5, pp.1513-1521, 2008.
[23] "dq theory applied to a permanent magnet synchronous machine with concentrated windings," by F. Meier and J. Soulard IET International Conference on Power Electronics, Machines and Drives (PEMD), pp. 194-198, 2008.
[24] Investigation on pole-slot combinations for permanent magnet machines with focused windings by F. Libert and J. Soulard International Conference on Electrical Machines (ICEM), 2004, CD-ROM.
[25] IEE Proc. on Electric Power Applications, vol. 151, no. 5, pp. 520-525, 2004; A.J. Mitcham, G. Antonopoulos, and J. Cullen, "Favorable slot and pole number combinations for fault-tolerant PM machines."
[26] Design considerations of a direct drive brushless machine with concentrated windings, R. Wrobel and P. Mellor, IEEE Trans. on Energy Conversion, vol. 23, no. 1, pp. 1-8, 2008.
[27] "Permanent magnet brushless machines with unequal tooth widths and similar slot and pole numbers," D. Ishak, Z.Q. Zhu, and D. Howe, IEEE Trans. on Industry Applications, vol.41, no.2, pp.584-590, 2005.
[28] "Influence of slot and pole numbers in brushless DC motors with unequal tooth widths," Journal of Applied Physics, vol.97, pp.10Q509-1~3 2005, D. Ishak, Z.Q. Zhu, and D. Howe.
[29] Z.Q. Zhu, D. Ishak, and D. Howe, "Modular permanent magnet brushless machines having a fractional number of slots per pole - Influence of stator teeth and back-irons," Proceedings of the 2006 International Conference on Electrical Machines and Systems (ICEMS2006), November 20–23, 2006, Nagasaki, Japan, CDROM, DS1F1-2, 4 pages.
[30] Analysis of rotor core losses in IPM machines by S. H. Han, T. M. Jahns, and Z. Q. Zhu, Proceedings of the 2008 IEEE Industry Applications Society Annual Meeting, October 5–9, 2008, Edmonton, Alberta, Canada, pp. 1–8, paper IAS44p2.
[31] "Design tradeoff between stator core losses and torque ripple in IPM machines," Proceedings of the 2008 IEEE Industry Applications Society, S. H. Han, T. M. Jahns, and Z. Q. Zhu
Annual Meeting, Edmonton, Alberta, Canada, October 5–9, 2008, pp. 1–8, paper IAS44p3.
[32] Z. Q. Zhu, D. Howe, and J. Mitchell, "Inductances and magnetic field analysis of brushless DC machines with surface-mounted magnets and non-overlapping stator windings," IEEE Trans. on Magnetics, vol. 31, no. 3, 1995.
[33] Z. Q. Zhu and D. Howe, "Winding inductance of brushless machines with surface mounted magnets," IEEE International Electric Machines and Drives Conference, pp. WB2/2.1-WB2/2.3, 1997.
[34] "Investigation of winding inductances in fractional slot surface-mounted permanent magnet brushless machines," A.M. El-Refaie, Z. Q. Zhu, T. M. Jahns, and D. Howe, Proceedings of the 2008 IEEE Industry Applications Society Annual Meeting, October 5–9, 2008, Edmonton, Alberta, Canada, pp. 1–8, paper IAS57p3.
[35]Power capabilities of salient pole PM synchronous motors in variable speed drive application, R.F. Schiferl and T.A. Lipo, IEEE Trans. on Industry Applications, vol.26, pp.115-123, 1990.
[36] Field-weakening performance of brushless synchronous AC motor drives, W.L. Soong and T.J.E. Miller, Proc. IEE-EPA, vol. 141, pp. 331-340, 1994.
[37]Z.Q. Zhu, Z.P. Xia, Y. F. Shi, D. Howe, A. Pride, and X.J. Chen, "Performance of Halbach magnetized brushless ac motor," IEEE Trans. Magnetics, vol.39, no.5, 2003, pp.2992-2994.
[38] "Optimal flux weakening in surface PM machines using concentrated windings," IEEE Trans. Industry Applications, vol. 41, pp. 790-800, 2005, A.M. EL-Refaie and T.M. Jahns.
[39] “Experimental verification of optimal flux weakening in surface PM machines using concentrated windings,” IEEE Trans. Industry Applications, vol. 42, pp. 443-453, 2006; A.M. EL-Refaie, T.M. Jahns, P.J. McCleer, and J.W. McKeever.
[40] A.M. "Scalability of surface PM machines with concentrated windings designed to achieve wide speed

ranges of constant-power operation," EL-Refaie and T. Jahns, IEEE Trans. on Energy Conversion, vol. 21, no. 2, pp. 362-369, 2005.
[41] C. Mecrow, A. G. Jack, and J. A. Haylock, "Fault tolerant permanent magnet motors drives," IEE Conference on Electrical Motors and Drives, pp. 433-437, 1995.
[42] G. Jack, B. C. Mecrow, and J. A. Haylock, "A comparative study of switched reluctance and permanent magnet motors for high-performance fault-tolerant applications," IEEE Trans. Industry Applications, vol. 32, no. 4, pp. 889-895, 1996.
[43] "Multi-phase fault-tolerant brushless DC motor drives," T. Gopalarathnam, H. A. Toliyat, and J. C. Moreira, Proc. IEEE Conf. on Industry Applications, vol. 3, pp. 1683-1688, 2000.
[44]J. D. Ede, K. Attalah, and D. Howe, "Design variations of modular permanent magnet brushless motor," Journal of Applied Physics, vol. 91, no. 10, pp. 6973-6975, 2002.
[45] N. Bianchi, M. Dai Pre, G. Grezzani, and S. Bolognani, "Design considerations on fractional-slot fault-tolerant synchronous motors," IEEE Int. Electrical Machines and Drives Conf. (IEMDC), May 2005, pp. 902-909.
[46]T. M. Jahns and W. L. Soong, "Pulsating torque minimization techniques for permanent magnet ac motor drives: a review," IEEE Trans. Industrial Electronics, vol. 43, no.2, pp. 321-330, 1996.
[47] Z.Q. Zhu and D. Howe, "Effect of design parameters on cogging torque in permanent magnet machines," IEEE Trans. Energy Conversion, vol. 15, no. 4, pp. 407-412, 2000.
[48] "Design techniques for reducing the cogging torque in surface-mounted PM motors," N. Bianchi and S. Bolognani, IEEE Trans. Industry Applications, vol. 38, no. 2, pp. 1259-1265, 2002.
[49] Z.Q. Zhu, S. Ruangsinchaiwanich, D. Ishak, and D. Howe, "Cogging torque analysis in brushless machines with stepped rotor and unevenly distributed stator slots"
magnets," IEEE Transactions on Magnetics, vol. 41, no. 10, pp. 3910-3912, 2005.
[50] Z. Q. Zhu, S. Ruangsinchaiwanich, Y. Chen, and D. Howe, "Evaluation of superimposition technique for calculating cogging torque in permanent magnet brushless machines," IEEE Trans. on Magnetics, vol.42, no.3, pp.1597-1603, 2006.
[51] "Minimization of cogging torque in axial flux permanent magnet machines – design concepts," IEEE Transactions on Magnetics, vol.43, no.9, pp.3614-3622, 2007; M. Aydin, Z. Q. Zhu, T. A. Lipo, and D. Howe.
[52] Z.Q. Zhu, Y.S. Chen, and D. Howe, "Iron loss in PM brushless ac machines under maximum torque per ampere and flux weakening control," IEEE Trans. on Magnetics, vol.38, no.5, pp.3285-3287, 2002.
[53] Iron loss in permanent magnet brushless machines with a fractional number of slots per pole, Z.Q. Zhu, D. Ishak, and D. Howe, Proceedings of the 2006 International Conference on Electrical Machines and Systems (ICEMS2006), November 20–23, 2006, Nagasaki, Japan, CDROM, DS1F1-3, 4 pages.
[54] Z. Q. Zhu, K. Ng, N. Schofield, and D. Howe, "Enhanced analytical modeling of rotor eddy current loss in brushless machines with surface-mounted permanent magnets," IEE Proc. EPA, vol. 151, no. 6, pp. 641-650, 2004.
[55] H. Polinder, M. Hoeijmakers, and M. Scuotto, "Eddy-Current Losses in the Solid Back-Iron of PM Machines for various Concentrated Fractional Pitch Windings," IEEE Int. Electric Machines and Drives Conf., vol. 1, pp.652-657, 2007.
[56]K. Atallah, D. Howe, P.H. Mellor, and D.A. Stone, "Rotor Loss in PM brushless AC machines," IEEE Trans. on Industry Applications, vol. 36, no. 6, pp. 1612-1618, 2000.
[57] Rotor eddy current loss in PM machines with fractional slot number per pole, D. Ishak, Z.Q. Zhu, and D. Howe, IEEE Trans. on Magnetics, vol.41, no.9, pp.2462-2469, 2005.
[58] "A general approach to determine the rotor losses in three-phase fractional-slot PM machines," N. Bianchi, S. Bolognani, and E. Fornasiero, Proceedings of the Electric Machines and Drives Conference (IEMDC), vol. 1, pp. 634-641, 2007.
[59]J. Ede, K. Atallah, G. Jewell, J. Wang, and D. Howe, "Axial segmentation of permanent magnets on rotor loss of modular brushless machines," IEEE Industry Applications Society Conf., vol. 3, pp. 1703-1708, 2004.
[60] Z. Q. Zhu, D. Ishak, D. Howe, and J.T. Chen, "Unbalanced magnetic forces in permanent magnet brushless machines with diametrically asymmetric disposition of phase windings," IEEE Trans. on Industry Applications, vol.43, no.6, pp.1544-1553, 2007.